PHYSICAL REVIEW B **67**, 165212 (2003)

Optical selection rules for shallow donors in 4H-SiC and ionization energy of the nitrogen donor at the hexagonal site

I. G. Ivanov, B. Magnusson, and E. Janzén

Department of Physics and Measurement Technology, Linköping University, S-581 83 Linköping, Sweden

(Received 9 December 2002; published 30 April 2003)

The selection rules for transitions between the electronic levels of shallow donors in 4H-SiC in the dipole approximation are derived. The ionization energy of the shallow nitrogen donor (at hexagonal site) is determined to be 61.4±0.5 meV by analyzing the photothermal ionization and infrared absorption spectra of nitrogen doped samples in the frame of model that approximates the effective-mass Hamiltonian in 4H-SiC with Hamiltonian of cylindric symmetry (Faulkner's model).

DOI: 10.1103/PhysRevB.67.165212 PACS number(s): 71.55.−i, 78.55.Hx

I. INTRODUCTION

In two recent publications,[1,2] data on the excited states of the shallower nitrogen donor, identified as nitrogen substituting for carbon atom at a hexagonal site N_h were published. These data obtained by photothermal ionization (PTI) spectroscopy[1] and infrared (IR) absorption[2] seem to be more reliable than older data based only on IR absorption,[3] mainly because of the much better quality of the sample used. Unfortunately, no identification of the observed donor excited states was attempted in these two publications, and the nitrogen binding energy for the shallower level was estimated to $E_{Dh}=60.2\pm0.5$ meV using only the temperature dependence of the spectrum.[1] In this paper, we provide such identification, based on the optical selection rules and on an estimate of the energies of the observed transitions obtained using Faulkner's model[4] as a suitable approximation. Since details concerning the symmetry of the wave functions and the optical selection rules in 4H-SiC seem to be absent in the literature, they are given in Sec. II. The comparison of the theoretical results with the experimental data is done in Sec. III, and the conclusions are summarized in Sec. IV.

II. THEORETICAL BACKGROUND AND GROUP-THEORETICAL INVESTIGATION OF THE OPTICAL SELECTION RULES

The conduction band of 4H-SiC has three equivalent minima (valleys) located at the M points of the Brillouin zone.[5] The group of the k vector for each of these points (valleys) is C_{2v}, with the C_2 axis oriented along the crystal c axis. The orientation of the coordinate system with respect to the crystal high-symmetry directions is shown in Fig. 1, together with some notations used further. Throughout this paper, we shall use the notations of Koster *et al.*[6] for the irreducible representations of the groups D_{2h} and C_{3v}. As for the group C_{2v}, also Koster's notations are used, but with the letter "M" instead of "Γ," in order to avoid confusion with the representations of C_{3v}.

As shown by Kohn and Luttinger,[7] the wave function of a shallow donor in the effective-mass approximation (EMA) can be presented in the form

$$\psi_k=\varphi_k'\varphi_k. \tag{1}$$

Here the index $k=1,2,3$ enumerates the equivalent minima, φ_k' is the free-electron (Bloch) wave function at the bottom of the conduction band, and φ_k is the envelope function, solution of the one-valley effective-mass Schrödinger equation. With our choice of coordinate system (see Fig. 1), the equation for the first valley (at the point $M^{(1)}$) becomes

$$H_1\varphi_1=-\frac{\hbar^2}{2}\left(\frac{1}{m_{\Gamma M}}\frac{\partial^2}{\partial x^2}+\frac{1}{m_{MK}}\frac{\partial^2}{\partial y^2}+\frac{1}{m_{ML}}\frac{\partial^2}{\partial z^2}+\frac{e^2}{\sqrt{\varepsilon_\perp\varepsilon_\parallel}\sqrt{x^2+y^2+(\varepsilon_\perp/\varepsilon_\parallel)z^2}}\right)\varphi_1=E\varphi_1. \tag{2}$$

Here H_1 denotes the effective-mass one-valley Hamiltonian, e is the electron charge, $\varepsilon_\parallel$ and $\varepsilon_\perp$ are the values of the

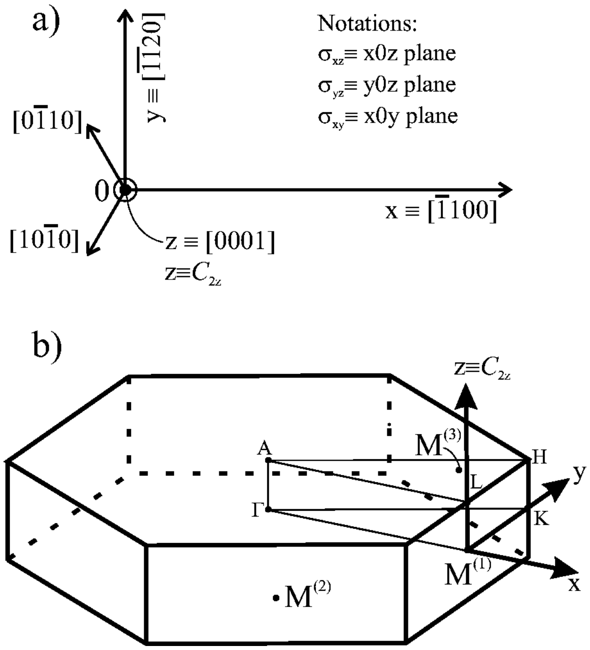

FIG. 1. Definition of some notations and the orientation of the Cartesian coordinate system with respect to (a) the crystal directions, and (b) the Brillouin zone. The three directions [$\bar{1}100$], [$0\bar{1}10$], and [$10\bar{1}0$] (enumerated 1,2 and 3, respectively) are the equivalent directions corresponding to **k**-vector at one of the three equivalent M-points ($M^{(1)}$, $M^{(2)}$, and $M^{(3)}$) in the Brillouin zone.

©2003 The American Physical Society

dielectric constant along and perpendicular to the c axis, respectively, and $m_{\Gamma M}$, m_{MK}, and m_{ML} are the electron effective masses along the high-symmetry directions $\Gamma-M$, $M-K$, and $M-L$ of the Brillouin zone, respectively. It is this equation that can be approximated by the Faulkner's model, if one substitutes for m_{ML} and m_{MK}, the average $m=\sqrt{m_{ML}m_{MK}}$, and sets the ratio $\varepsilon_\perp/\varepsilon_\parallel=1$ (the real value in both 4H- and 6H-SiC seems to be about 0.96),[8,9] thus neglecting the anisotropy of the dielectric tensor. The approximation for m_{ML} and m_{MK} is justified (only for 4H-SiC) by the measured values of the effective mass tensor, namely, $m_{\Gamma M}=0.58\pm0.1$, $m_{ML}=0.33\pm0.1$, and $m_{MK}=0.31\pm0.1$ (in units of the rest mass of electron).[10] Within these approximations, Eq. (2) transforms to the form given in Ref. 4. The usefulness of such approximations is that a good estimation for energies of the donor states can be obtained simply by interpolation from Faulkner's tables. For the interpolation, it will be natural to use the values (in Faulkner's notations)[4] $m_\perp=\sqrt{(m_{ML}m_{MK})}=0.32$ and $m_\parallel=m_{\Gamma M}=0.58$. The Faulkner's parameter is $\gamma^{1/3}=(m_\perp/m_\parallel)^{1/3}=0.82$ in this case. For $\varepsilon=\sqrt{\varepsilon_\parallel\varepsilon_\perp}$, we take the value $\varepsilon=9.95$.[9]

Note that the Hamiltonian used in Ref. 4 has cylindrical symmetry $D_{\infty h}$, whereas in the case of 4H-SiC (or any other hexagonal polytype of SiC) the symmetry is D_{2h}, according to Eq. (2). Hence, φ_k will be classified according to the irreducible representations of D_{2h}.

The correspondence between the states presented in Ref. 4 and the states of the Hamiltonian in Eq. (2) is easily established. The S-like states[4] (or, shortly, S states) are those that possess the full symmetry of D_{2h}, i.e., transform as Γ_1^+. The quantization axis for the orbital momentum l is Ox in our case, hence the classification by parity holds with respect to the σ_{yz} plane. The P_0-like (or simply P_0) states have odd parity, i.e. the corresponding wave function changes sign after reflection in σ_{yz}. One easily finds that they transform according to Γ_4^- in D_{2h}. The $P_\pm$-like (odd parity) states are degenerate only in $D_{\infty h}$ symmetry. In D_{2h}, they will split into two (closely spaced) states, which we call for convenience P_y and P_z states (sign changes after reflection in σ_{xz} for the former, and σ_{xy} for the latter). Hence, P_y states transform as Γ_2^-, and P_z states as Γ_3^- irreducible representations of D_{2h}. Both these states are approximated by the corresponding $P_\pm$ state from Faulkner's model, because the deviation of the Hamiltonian in Eq. (2) from cylindrical symmetry is small. Since the enumerated states are most important for comparison with the experiment and represent the lowest lying states, our derivation of selection rules will be restricted to transitions between them.

The transformation properties of φ_k in C_{2v} (which is a subgroup of D_{2h}) are found simply by comparing the representations of these two groups, and one obtains that each product function ψ_k $(k=1,2,3)$, as defined in Eq. (1), transforms as M_4 for S and P_z states, as M_1 for P_y states, and as M_3 for P_0 states. The transformation properties of the one-valley wave functions ψ_k and the Faulkner's states corresponding to them are summarized in Table I. The transformation properties of ψ_k in the group C_2 are also shown, since they will be needed later on. The notations Γ^+ and Γ^- will also be defined later.

TABLE I. Symmetry of the one-valley wave functions ψ_k in C_{2v}, and their relation to Faulkner's states. The main quantum number n is $n\geqslant1$ for the S states, and $n\geqslant2$ for the other states.

Type of ψ_k	Symmetry In C_{2v}	In C_2	Approximated by[a]
nS state	M_4	Γ^-	nS
nP_0 state	M_3	Γ^+	nP_0
nP_y state	M_1	Γ^+	$nP_\pm$
nP_z state	M_4	Γ^-	$nP_\pm$

[a] Denotes the corresponding state within the Faulkner's model (Ref. 4), used to approximate the binding energy.

The site symmetry of substitutional donor in 4H-SiC is C_{3v}. The three functions ψ_k $(k=1,2,3)$ corresponding to certain energy eigenvalue of Eq. (2) must form a basis for a representation Γ of C_{3v},[7] called here the wave function representation. The total wave function Ψ of the donor electron in the EMA is, in general, a linear combination of the wave functions ψ_k corresponding to the three valleys,

$$\Psi=a_1\psi_1+a_2\psi_2+a_3\psi_3, \tag{3}$$

and, therefore, transforms according to the wave function representation Γ. The latter can be deduced in a standard way from the transformation properties of ψ_k under the symmetry operations of C_{3v}. It is a three-dimensional reducible representation, which can be presented as a direct sum of the irreducible representations of C_{3v}. The result is that if the basis functions ψ_k have M_4 or M_3 symmetry in C_{2v} (nS, nP_z, and nP_0 states), then $\Gamma=\Gamma_2+\Gamma_3$, whereas if ψ_k transforms as M_1 (nP_y states), $\Gamma=\Gamma_1+\Gamma_3$. Therefore, each state splits into one nondegenerate (Γ_1 or Γ_2), and one double-degenerate (Γ_3) state. The splitting is a consequence of the valley-orbit interaction, which is usually not accounted for by the EMA.[7]

The coefficients a_k, $k=1,2,3$, in Eq. (3) can be found for each irreducible representation using standard projection-operators technique.[11] The results, presented shortly in the form (a_1,a_2,a_3) are, as follows:

$(1/\sqrt{3},1/\sqrt{3},1/\sqrt{3})$ for both Γ_1 or Γ_2;

$1/\sqrt{6}(2,-1,-1)$ for the first row of Γ_3;

$1/\sqrt{2}(0,1,-1)$ for the second row of Γ_3.

We note also that all wave functions have zero amplitude at the donor nucleus, which follows from Eq. (1) and the M_4 symmetry of φ_k'.

At low temperatures, usually only the donor ground state and possibly its valley-orbit split-off counterpart are populated. In our notations, these are the two states $1S(\Gamma_2)$ and $1S(\Gamma_3)$, and it has been shown for the N-donor, that $1S(\Gamma_2)$ is the ground state.[12] One of these two states is always the initial state Ψ_i in absorption, and we consider now the selection rules for matrix elements of the form $(\Psi_f,V\Psi_i)$, responsible for the transitions. In C_{3v}, the dipole operator V transforms as Γ_3 for polarization $E\perp c$ (i.e., perpendicular to the crystal axis), and as Γ_1 for $E\parallel c$.[12] Therefore, for $E\parallel c$ the function $V\Psi_i$ transforms as Ψ_i, which means that transitions from $1S(\Gamma_2)$ (the ground state) are allowed only to other states with Γ_2 symmetry, namely, to $nS(\Gamma_2)$, $nP_0(\Gamma_2)$, and $nP_z(\Gamma_2)$ states with $n \geqslant 2$. Transitions from $1S(\Gamma_3)$ with $E \| c$ are allowed to the Γ_3 split-off counterpart of all states. For $E \perp c$, and if the initial state Ψ_i is the ground $1S(\Gamma_2)$ state, then $V\Psi_i$ has $\Gamma_3 \otimes \Gamma_2 = \Gamma_3$ symmetry. Hence, transitions to the Γ_3 counterpart of all excited states are allowed. For the $1S(\Gamma_3)$ state, $V\Psi_i$ has $\Gamma_3 \otimes \Gamma_3 = \Gamma_1 + \Gamma_2 + \Gamma_3$ symmetry, and transitions to all states are allowed.

However, the selection rules considered only within the C_{3v} symmetry are not sufficient to find all forbidden transitions. Indeed, by virtue of Eq. (3), each matrix element is a sum of subelements of the form

$$(a_m)_f^p (a_n)_i^q ((\psi_m)_f^p, V(\psi_n)_i^q), \tag{4}$$

where the coefficients a_m, a_n and the one-valley wave functions ψ_m, ψ_n are labeled with the number (p or q) of the respective irreducible representation [superscript p for the final f, and q for the initial i state]. The selection rules in C_{3v} give the sums of such terms that do not vanish, provided that at least one of the subelements in the sum is not zero. However, by considering the symmetry of the constituting matrix elements $((\psi_m)_f^p, V(\psi_n)_i^q)$, one finds additional selection rules.

We consider first the terms with $m = n$ representing transitions within one valley, i.e., $((\psi_n)_f^p, V(\psi_n)_i^q)$ (we will call them shortly "diagonal terms"). Obviously, the selection rules for the diagonal terms can be established for only one of them [say, $((\psi_1)_f^p, V(\psi_1)_i^q)$], and this can be done entirely in the environment of C_{2v} symmetry. The dipole operator V always transforms as the rows of the three-dimensional rotational representation R, which in C_{2v} is readily in diagonal form, $R = M_2 + M_4 + M_1$. Then it is convenient to consider the three polarizations $E \| Ox$, $E \| Oy$, and $E \| Oz$ separately, because they transform as M_2, M_4, and M_1, respectively. Since the initial state $(\psi_1)_i^q$ always transforms as M_4 [i.e., $q = M_4$ for both $1S(\Gamma_2)$ and $1S(\Gamma_3)$], the final state $(\psi_1)_f^p$ must transform as $M_2 \otimes M_4 = M_3$ for $E \| Ox$, $M_4 \otimes M_4 = M_1$ for $E \| Oy$, and $M_1 \otimes M_4 = M_4$ for $E \| Oz$. The former two selection rules correspond to light polarized $E \perp c$ and can be combined into a single one, namely, transitions from initial state of M_4 symmetry are possible only to states of M_3 and M_1 symmetries (i.e., nP_0 and nP_y, see Table I). The last selection rule corresponds to light polarized $E \| c$ and shows that in this case only transitions to states with the same symmetry as the initial state M_4 are allowed (i.e., nS and nP_z).

Let us consider now the off-diagonal terms $(m \neq n)$. It is easily deduced from Fig. 1 that the one-valley wave functions $(\psi_m)_f^p$ and $(\psi_n)_i^q$ with $m \neq n$ have only two common symmetry elements, namely, the identity operation E and the twofold rotation C_{2z} about the z axis. In other words, the intersection group of the three C_{2v} groups corresponding to the three equivalent valleys $M^{(1)}$, $M^{(2)}$, and $M^{(3)}$ is simply C_2, a subgroup of C_{2v}. C_2 has two one-dimensional irreducible representations, denoted here as Γ^+ (the trivial representation), and Γ^- (with matrices "1" for E, and "-1" for C_{2z}). The transformation properties of ψ_k in the C_2 symmetry are shown in Table I. According to the compatibility relations, the irreducible representations M_2 and M_4 in C_{2v} correspond to Γ^- in C_2, whereas M_1 and M_3 correspond to Γ^+. Therefore, the dipole operator V transforms as Γ^- for $E \perp c$, and as Γ^+ for $E \| c$. The wave function of the initial state $(\psi_n)_i^{M_4}$ always transforms as Γ^-, according to Table I. Hence, $V(\psi_n)_i^{M_4}$ transforms as $\Gamma^- \otimes \Gamma^- = \Gamma^+$ for $E \perp c$, and as $\Gamma^+ \otimes \Gamma^- = \Gamma^-$ for $E \| c$. Consequently, for $E \perp c$, the off-diagonal elements are nonzero only if the final state transforms as Γ^+. According to Table I, the allowed final states are nP_0 and nP_y in this case. For $E \| c$, the final state must have Γ^- symmetry in C_2, which selects nS and nP_z as possible final states (see Table I). Comparing these results with the results for the diagonal matrix elements, we notice that there are cases when the diagonal elements vanish, but the off-diagonal elements do not. However, this does not change the selection rules deduced by considering only the diagonal terms. For example, for $E \perp c$, transitions were allowed only to states transforming as M_1 and M_3, but these are exactly the states transforming as Γ^+ in C_2 (nP_0 and nP_y). The same holds for $E \| c$, the diagonal terms were nonzero only for final states of M_4 symmetry, but these are also the states transforming as Γ^- in C_2 (nS and nP_z). Combining the selection rules deduced for the constituting matrix elements from Eq. (4) with the selection rules in C_{3v}, we obtain the final selection rules presented in Table II.

TABLE II. Selection rules in 4H-SiC for optical transitions from the ground state $1S(\Gamma_2)$ and its valley-orbit split-off counterpart $1S(\Gamma_3)$ to other excited states.

Initial state	Allowed final states ($n \geqslant 2$)
Polarization $E \perp c$	
$1S(\Gamma_2)$	$nP_0(\Gamma_3)$, $nP_y(\Gamma_3)$
$1S(\Gamma_3)$	$nP_y(\Gamma_1)$, $nP_0(\Gamma_3)$, $nP_0(\Gamma_2)$, $nP_y(\Gamma_3)$
Polarization $E \| c$	
$1S(\Gamma_2)$	$nS(\Gamma_2)$, $nP_z(\Gamma_2)$
$1S(\Gamma_3)$	$nS(\Gamma_3)$, $nP_z(\Gamma_3)$

III. COMPARISON WITH THE EXPERIMENTAL DATA AND DISCUSSION

We compare now the energy levels calculated with Faulkner's model to the experimental data. This is done in Table III and Fig. 2, displaying our own photothermal ionization spectrum of a 4H-SiC sample.

We have to clarify the way the theoretical values presented in Table III were obtained. The theoretical binding energies for the final state of each transition were calculated using Faulkner's model, as described in Sec. II. It is well known that the effective-mass theory describes well the excited states, but fails to describe the ground state (as well as its valley-orbit splitting, of course). Thus, the theoretical value for the binding energy of the 1S state (i.e., the theoretical donor ionization energy) calculated with our choice of parameters (see Sec. II) is 53.1 meV, which is assumed to be inaccurate. [This value is the common theoretical estimate for both $1S(\Gamma_2)$ and $1S(\Gamma_3)$ states.] Therefore, the theoret-

TABLE III. Identification of the transitions between the levels of the shallow donor N_h observed in the PTI spectra, and comparison of the experimental energy values with the calculated ones. All energy units are meV.

	Experimental		Theoretical	
Transition	Energy [a]	Energy [b]	Binding energy [c]	Transition energy [d]
Polarization $E\perp c$				
$1S(\Gamma_3)-2P_0(\Gamma_2,\Gamma_3)$	38.1	38.2	15.53	38.47
$1S(\Gamma_3)-2P_y(\Gamma_1,\Gamma_3)$	41.8	41.8	12.27	41.73
$1S(\Gamma_2)-2P_0(\Gamma_3)$	45.6	45.6	15.53	45.87
$1S(\Gamma_3)-3P_0(\Gamma_2,\Gamma_3)$		46.8	6.99	47.01
$1S(\Gamma_3)-3P_y(\Gamma_1,\Gamma_3)$	48.4	~48.5	5.52	48.48
$1S(\Gamma_2)-2P_y(\Gamma_3)$	49.2	49.2	12.27	49.13
$1S(\Gamma_2)-3P_0(\Gamma_3)$	54.2	shoulder~54.7	6.99	54.41
$1S(\Gamma_2)-3P_y(\Gamma_3)$	55.9−56.3	55.9	5.52	55.88
Polarization $E\parallel c$				
$1S(\Gamma_2)-2S(\Gamma_2)$	48.1		13.53	47.87
$1S(\Gamma_3)-2S(\Gamma_3)$	40.7		13.53	40.52

[a] Values from Refs. 1,2, converted to meV.

[b] Values from our measurement, see Fig. 2.

[c] The binding energy of the final state, calculated with Faulkner's model.

[d] Calculated for each state as explained in text.

ical transition energies *cannot* be calculated by subtracting the binding energy of the final state from the *theoretical* ionization energy. The transition energies can be calculated by subtracting the calculated binding energies of the final states from some empirical value for the binding energy of either the $1S(\Gamma_2)$, or the $1S(\Gamma_3)$ state. These latter values are chosen in such way as to provide the best match between the calculated and the observed transition energies. The energies of 61.40 meV for the $1S(\Gamma_2)$ state, and 54.00 meV for the $1S(\Gamma_3)$ state are chosen to calculate the transition energies presented in the last column of Table III. The former energy is the donor ionization energy. The difference between these two energies, 7.41 meV, is in close agreement with the value of the valley-orbit splitting of the ground state (7.4 meV), determined previously.[1]

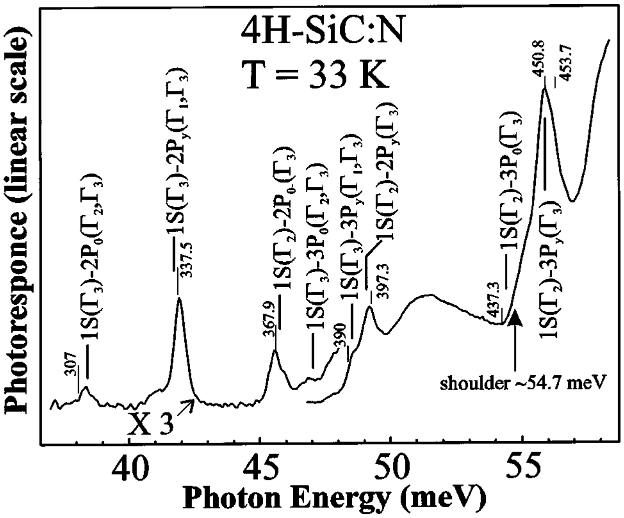

FIG. 2. Spectrum of the photocurrent vs incident photon energy for a sample of 4*H*-SiC:N. The bars labeled with numbers denote the positions of the lines observed in Ref. 1, the numbers being the corresponding photon energies in cm^{-1}. The rest of the bars are at the calculated energies for the transitions from either the $1S(\Gamma_2)$ ground state, or the $1S(\Gamma_3)$ valley-orbit split-off state to the excited state, as denoted for each bar.

The agreement between the model and experiment is excellent, thus the model provides also identification of the lines. Table III compares to the theory also the transitions induced by light with $E\parallel c$, observed in IR absorption,[2] and associated here with $1S(\Gamma_2)-2S(\Gamma_2)$ and $1S(\Gamma_3)-2S(\Gamma_3)$ transitions. The separation between these two absorption peaks (7.4 meV) corresponds to the sum of the valley-orbit splitting of the $1S$ and $2S$ states, according to their identification. On the other hand, in the preceding paragraph, we saw that 7.4 meV can be attributed to the valley-orbit splitting of the $1S$ state alone, i.e., the separation between $1S(\Gamma_2)$ and $1S(\Gamma_3)$. This leads us to the conclusion that the valley-orbit splitting of the $2S$ state is much smaller than for the $1S$ state, probably within the experimental error ($\lesssim 0.5$ meV, approximately). Moreover, several peaks in the PTI spectrum are expected to be doublets with splitting equal to the valley-orbit splitting of the involved excited state. Consider for example the peaks at 45.6 and 38.1 meV. The former is identified as $1S(\Gamma_3)-2P_0(\Gamma_2,\Gamma_3)$ (doublet), and the latter as $1S(\Gamma_2)-2P_0(\Gamma_3)$ (singlet) transitions. The doublet is not observed, however, either because one of its components is very weak, or because its valley-orbit splitting is too small to be resolved experimentally, which is the most probable reason. This leads us to conclude that the valley-orbit splitting is negligible for all states except $1S$.

The overall agreement of the two experimental sets of data obtained with $E\perp c$ is obvious, however, small discrepancies beyond the experimental error can be noticed, especially in the transitions to higher excited states. For example, the line at 437.3 cm^{-1} (54.22 meV) from Ref. 1 can be observed as a shoulder around 54.7 meV, on the left side of the peak at 56 meV (see Fig. 2). Also, the splitting of this latter peak is not observed in our spectra. These small discrepancies may be due to the different stress conditions in our sample from the one used in Ref. 1, to which the excited states will be more sensitive due to their larger orbits. We note also that the weak peak at 46.8 meV, associated with the $1S(\Gamma_3)-3P_0(\Gamma_2,\Gamma_3)$ transition was not reported in Ref. 1. Otherwise, the discrepancy between the theoretical model and the experiment (both sets of data) does not exceed 0.3 meV (see Table III). We conclude that, apart from the simplicity of the model, the disagreement between theory and experiment is due at least to some extent to the stress present in the samples. However, the model describes very well the observed levels, and yields the ionization energy of the nitrogen donor at hexagonal site, $E_{Dh}=61.4\pm0.5$ meV. This value is close to the 60.2 meV determined in Ref. 1 on the base of the temperature dependence of the photoionization spectrum, but we consider our value as more accurate.

Transitions to P_z states are allowed with $E\|c$ but not observed, probably due to low oscillator strength. The behavior of the Bloch wave functions φ_k' needs to be known in order to make possible the estimation of the relative intensities of the lines. In this connection, it is worth pointing out that if φ_k' are either symmetric, or asymmetric with respect to the plane σ_{xy}, i.e., if $\varphi_k'(x,y,z)=\pm\varphi_k'(x,y,-z)$, transitions between the S states for polarization $E\|c$ become forbidden. In such case the only allowed transitions with $E\|c$ from the ground donor state would be to P_z states, which, similar to P_y states, are also approximated by the $P_{\pm}$-like states from Faulkner's model. Our assignment to transitions between S states in Table III for $E\|c$ is based entirely on the match between the measured peak energy and the calculated one. However, the measured peaks in the IR absorption are more than 2 meV broad (see Ref. 2), probably indicating poor sample quality. Thus more experimental work on better material, as well as more advanced theory will be needed in order to decide conclusively on the nature of these peaks.

Finally, we would like to comment on an earlier work,[3] which also attempts interpretation of the N-donor excited states observed in infrared absorption. The authors apply the model suggested by Gerlach and Pollmann,[13] which accounts for the anisotropy of ε. At the time of this publication, the electron effective masses were not known, so a fitting procedure is used for determination of a longitudinal and transversal effective masses, required to apply the theory. However, their values disagree with the recently measured electron effective mass tensor.[10] These latter values are in good agreement with the theory,[5] and from them it follows that the Gerlach-Pollmann model is *not* applicable to $4H$-SiC. Indeed, their model requires that the anisotropy of ε and the effective mass tensor are along the same axis (z axis in Ref. 13), whereas in $4H$-SiC, the large effective mass anisotropy is along the x axis, while the anisotropy of ε is along the z axis ($\equiv c$ axis). The theory has not been worked out for the case of Eq. (2), and since the anisotropy of ε is usually small, it is not surprising that we obtain a better agreement with the data by neglecting it, and then applying Faulkner's theory with no adjustable parameters.

IV. CONCLUSIONS

We have shown that the experimental data on the excited states of the nitrogen donor at hexagonal site in $4H$-SiC are described very well with the Faulkner's model,[4] using the data for the electron effective-mass tensor from Ref. 10. Since no adjustable parameters have been used in the model, the agreement between theory and experiment serves as an indirect confirmation of the accuracy of the experimentally determined electron effective masses.[10] The optical selection rules deduced here are also in agreement with the experimental data, and we are able to conclude that the valley-orbit splitting of the donor states in $4H$-SiC is only important for the ground state. Its value is probably too small to be observed for the excited states, at least as long as measurements on $4H$-SiC material of the present quality are considered.

ACKNOWLEDGMENTS

We thank professor U. Lindefelt for many useful discussions on group theory. Support from the SSF program SiCEP and the Swedish Research Council is gratefully acknowledged.

---

[1] C.Q. Chen, J. Zeman, F. Engelbrecht, C. Peppermüller, R. Helbig, Z.H. Chen, and G. Martinez, J. Appl. Phys. **87**, 3800 (2000).

[2] C.Q. Chen, R. Helbig, F. Engelbrecht, and J. Zeman, Appl. Phys. A: Mater. Sci. Process. **A72**, 717 (2001).

[3] W. Götz, A. Schöner, G. Pensl, W. Suttrop, W.J. Choyke, R. Stein, and S. Leibenzeder, J. Appl. Phys. **73**, 3332 (1993).

[4] R.A. Faulkner, Phys. Rev. **184**, 713 (1969).

[5] C. Persson and U. Lindefelt, J. Appl. Phys. **82**, 5496 (1997).

[6] G.F. Koster, J.O. Dimmock, R.G. Wheeler, and H. Statz, *Properties of the Thirty-Two Point Groups* (MIT Press, Cambridge, 1963).

[7] W. Kohn and J.M. Luttinger, Phys. Rev. **98**, 915 (1955).

[8] W.J. Choyke and L. Patrick, Phys. Rev. B **2**, 2255 (1970).

[9] I.G. Ivanov, B. Magnusson, and E. Janzén, Phys. Rev. B **67**, 165211 (2003).

[10] D. Volm, B.K. Meyer, D.M. Hofmann, W.M. Chen, N.T. Son, C. Persson, U. Lindefelt, O. Kordina, E. Sörman, A.O. Konstantinov, B. Monemar, and E. Janzén, Phys. Rev. B **53**, 15 409 (1996).

[11] See, e.g., J.F. Cornwell, in *Group Theory and Electronic Energy Bands in Solids*, edited by E.P. Wohlfarth (North-Holland, Amsterdam, 1969).

[12] I.G. Ivanov, U. Lindefelt, A. Henry, O. Kordina, C. Hallin, M. Aroyo, T. Egilsson, and E. Janzén, Phys. Rev. B **58**, 13 634 (1998).

[13] B. Gerlach and J. Pollmann, Phys. Status Solidi B **67**, 93 (1975).